VOLUME 91, NUMBER 11 PHYSICAL REVIEW LETTERS week ending 12 SEPTEMBER 2003

Nucleon-Nucleon Coincidence Spectra in the Nonmesonic Weak Decay of Λ Hypernuclei and the Γ_n/Γ_p Puzzle

G. Garbarino, A. Parreño, and A. Ramos

Departament d'Estructura i Constituents de la Matèria, Universitat de Barcelona, E-08028 Barcelona, Spain

(Received 17 January 2003; published 9 September 2003)

By combining a one-meson-exchange model for the $\Lambda N \to nN$ transition in finite nuclei with an intranuclear cascade code, we have obtained nucleon-nucleon (angular and energy) coincidence distributions from the nonmesonic weak decay of ${}^{5}_{\Lambda}\mathrm{He}$ and ${}^{12}_{\Lambda}\mathrm{C}$ hypernuclei. Although, due to the elimination of interferences, two-nucleon coincidences are expected to give a cleaner extraction (with respect to single nucleon observables) of the ratio $\Gamma_n/\Gamma_p \equiv \Gamma(\Lambda n \to nn)/\Gamma(\Lambda p \to np)$, we show that the effect of the final state interactions is still important even when applying favorable energy and angular cuts. The agreement of our results for the ratio N_{nn}/N_{np} between the number of nn and np emitted pairs with preliminary KEK coincidence data allows us to conclude that Γ_n/Γ_p for ${}^{5}_{\Lambda}\mathrm{He}$ should be small and close to the value of 0.46 predicted by our meson-exchange model.

DOI: 10.1103/PhysRevLett.91.112501 PACS numbers: 21.80.+a, 13.30.Eg, 13.75.Ev

For many years, a sound theoretical explanation of the large experimental values of the ratio, Γ_n/Γ_p, between the neutron- and proton-induced nonmesonic decay widths, $\Gamma(\Lambda n \to nn)$ and $\Gamma(\Lambda p \to np)$, of Λ hypernuclei has been missing [1,2]. The calculations underestimate the central data for all considered hypernuclei, although the large experimental error bars do not allow one to reach any definite conclusion. Because of its strong tensor component, the one-pion-exchange (OPE) model with the $\Delta I = 1/2$ isospin rule supplies very small ratios, typically in the interval 0.05–0.20. On the contrary, the OPE description can reproduce the total nonmesonic decay rates observed for light and medium hypernuclei. Other interaction mechanisms beyond OPE might then be responsible for the overestimation of Γ_p and the underestimation of Γ_n. Among these, the most relevant are (i) the inclusion in the $\Lambda N \to nN$ transition potential of mesons heavier than the pion (also including the exchange of correlated or uncorrelated two pions) [3–7]; (ii) the inclusion of interaction terms that explicitly violate the $\Delta I = 1/2$ rule [1,8,9]; (iii) the inclusion of the two-body induced decay mechanism [10–13]; and (iv) the description of the short range $\Lambda N \to nN$ transition in terms of quark degrees of freedom [14,15], which automatically introduces $\Delta I = 3/2$ contributions.

Recent progress has been made on the subject.

(i) On the one hand, a few calculations [5–7,14] zwith $\Lambda N \to nN$ transition potentials including heavy-meson-exchange and/or direct quark contributions obtained ratios more in agreement with data, without providing, nevertheless, a satisfactory explanation of the puzzle [1].

(ii) On the other hand, an error in the computer program employed in Ref. [16] to evaluate the single nucleon energy spectra from nonmesonic decay has been corrected [17], leading to quite different spectral shapes, which, once compared with old experimental data for ${}^{12}_{\Lambda}\mathrm{C}$ [18], allowed one to extract smaller values of Γ_n/Γ_p.

In the light of these recent developments and of new experiments [19–21], it is important to develop different theoretical approaches and strategies for the determination of the Γ_n/Γ_p ratio. In this Letter we present a finite nucleus calculation of the nucleon-nucleon coincidence distributions in the nonmesonic weak decay of ${}^{5}_{\Lambda}\mathrm{He}$ and ${}^{12}_{\Lambda}\mathrm{C}$ hypernuclei. The work is motivated by the fact that correlation observables permit a *cleaner* extraction of Γ_n/Γ_p from the data. This is due to the elimination of some interference terms between n- and p-induced mechanisms [1], which are unavoidable in experimental data but that cannot be taken into account by the Monte Carlo methods usually employed to simulate the nucleon final state interactions. An experiment performed very recently at KEK [19] has actually measured the angular and energy correlations that we discuss in this paper. Some preliminary results of the experiment can already be compared with our calculations.

The one-meson-exchange (OME) weak transition potential we employ to describe the one-nucleon stimulated decays contains the exchange of ρ, K, K^*, ω, and η mesons in addition to the pion [4,6]. The final state interactions acting between the two primary nucleons are taken into account by using a scattering NN wave function from the Lippmann-Schwinger (T matrix) equation obtained with the NSC97f potential [22]. The decay rates predicted by this OME model (in units of the free Λ decay width) are the following ones [6]: $\Gamma_1 \equiv \Gamma_n + \Gamma_p = 0.32$, $\Gamma_n/\Gamma_p = 0.46$ for ${}^{5}_{\Lambda}\mathrm{He}$, and $\Gamma_1 = 0.55$, $\Gamma_n/\Gamma_p = 0.34$ for ${}^{12}_{\Lambda}\mathrm{C}$.

In the present work, the rate and distributions of primary nucleons from the two-nucleon induced process, $\Lambda np \to nnp$, are taken from those obtained with the polarization propagator method in the local density

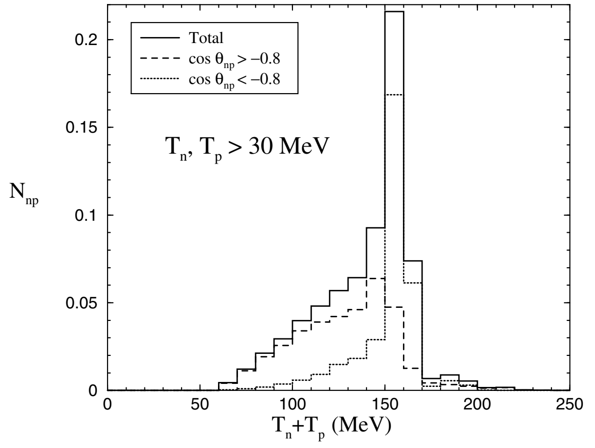

FIG. 1. Kinetic energy correlations of np pairs emitted *per nonmesonic decay* of $^{5}_{\Lambda}\mathrm{He}$. See text for details.

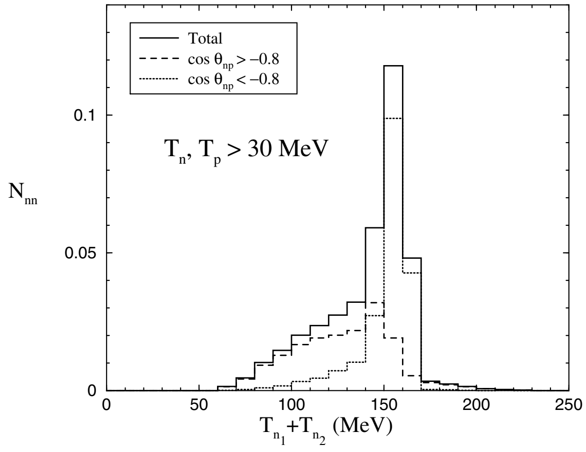

FIG. 2. Kinetic energy correlations of nn pairs emitted *per nonmesonic decay* of $^{5}_{\Lambda}\mathrm{He}$. See text for details.

approximation of Ref. [12], properly scaled to maintain the ratio Γ_2/Γ_1 unchanged, namely, $\Gamma_2/\Gamma_1 = (\Gamma_2/\Gamma_1)^{\mathrm{LDA}} = 0.20$ for $^{5}_{\Lambda}\mathrm{He}$ and 0.25 for $^{12}_{\Lambda}\mathrm{C}$ [23].

In their way out of the nucleus, the primary nucleons, due to collisions with other nucleons, continuously change energy, direction, and charge. As a consequence, secondary nucleons are also emitted. We simulate the nucleon propagation inside the residual nucleus with the intranuclear cascade code of Ref. [16], which can be easily applied to primary nucleon distributions originated by any of the proposed weak decay models [3–8,10–15]. We are aware of the fact that accounting for nucleon final state interaction (FSI) effects in light residual nuclei through Monte Carlo techniques is questionable. For this reason, the results for $^{5}_{\Lambda}\mathrm{He}$ should be considered as less realistic than the corresponding ones for $^{12}_{\Lambda}\mathrm{C}$.

In Fig. 1 we show the kinetic energy correlation of np coincidence pairs emitted in the nonmesonic decay of $^{5}_{\Lambda}\mathrm{He}$. The spectra are normalized *per nonmesonic weak decay.* To facilitate a comparison with experiments, whose kinetic energy threshold for proton (neutron) detection is typically of about 30 (10) MeV, and to avoid a possible nonrealistic behavior of the intranuclear cascade simulation for low nucleon energies, in all the figures of the paper we required T_n, $T_p \geq 30$ MeV. A narrow peak is predicted close to the Q value (153 MeV) expected for the proton-induced three-body process $^{5}_{\Lambda}\mathrm{He} \rightarrow {}^{3}\mathrm{H} + n + p$: it is mainly originated by the back-to-back kinematics ($\cos\theta_{np} < -0.8$). A broad peak, predominantly due to $\Lambda p \rightarrow np$ or $\Lambda n \rightarrow nn$ weak transitions followed by the emission of secondary (less energetic) nucleons, has been found around 140 MeV for $\cos\theta_{np} > -0.8$. The kinetic energy correlation for $^{5}_{\Lambda}\mathrm{He}$ nn pairs (Fig. 2) shows essentially the same structure of the np distribution just discussed.

In Fig. 3, which corresponds to the energy correlation of $^{12}_{\Lambda}\mathrm{C}$ np pairs, the narrow peak appearing at $T_n + T_p \simeq 155$ MeV again gets the dominant contribution from back-to-back coincidences. The relevance of the nucleon FSI in $^{12}_{\Lambda}\mathrm{C}$ relative to $^{5}_{\Lambda}\mathrm{He}$ can be seen from the second, broader peak appearing in the region around 110 MeV for $^{12}_{\Lambda}\mathrm{C}$ and 140 MeV for $^{5}_{\Lambda}\mathrm{He}$. This peak is in fact more pronounced for the heavier hypernucleus. Another consequence of the different FSI effects in $^{5}_{\Lambda}\mathrm{He}$ and $^{12}_{\Lambda}\mathrm{C}$ is the different magnitude of the tail of the back-to-back distribution at low energies.

Figures 4 and 5 show the opening angle correlations of nn, np, and pp pairs emitted in the decay of $^{5}_{\Lambda}\mathrm{He}$ and $^{12}_{\Lambda}\mathrm{C}$, respectively. Comparing both figures for nn and np, one sees that the back-to-back peaks are more pronounced for $^{5}_{\Lambda}\mathrm{He}$ (less sensitive to FSI) than for $^{12}_{\Lambda}\mathrm{C}$, while the (almost uniform) tail of these distributions (fed by FSI) is more significant in $^{12}_{\Lambda}\mathrm{C}$ than in $^{5}_{\Lambda}\mathrm{He}$. Since at least one proton of any pp coincidence is a secondary particle, the pp spectra are quite uniform: actually, due to the relevance of the back-to-back kinematics in the weak decay, these distributions slowly decrease as $\cos\theta_{pp}$ increases. Again as a

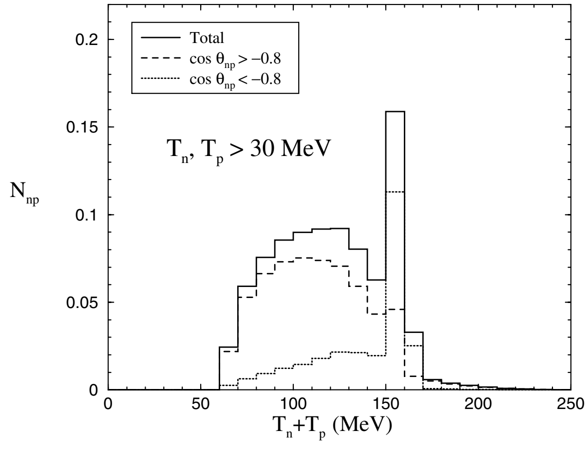

FIG. 3. Kinetic energy correlations of np pairs emitted *per nonmesonic decay* of $^{12}_{\Lambda}\mathrm{C}$. See text for details.

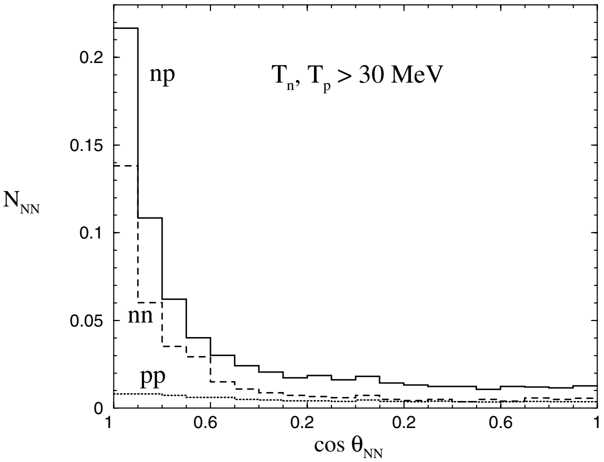

FIG. 4. Opening angle correlations of *nn*, *np*, and *pp* pairs emitted *per nonmesonic decay* of ${}^{5}_{\Lambda}$He. See text for details.

consequence of FSI, the number of *pp* pairs is considerably larger in ${}^{12}_{\Lambda}$C than in ${}^{5}_{\Lambda}$He.

The ratio Γ_n/Γ_p is defined as the ratio between the number of primary weak decay *nn* and *np* pairs, $N_{nn}^{\rm wd}$ and $N_{np}^{\rm wd}$. However, due to two-body induced decays and nucleon FSI, one expects the inequality

$$\frac{\Gamma_n}{\Gamma_p} \equiv \frac{N_{nn}^{\rm wd}}{N_{np}^{\rm wd}} \neq \frac{N_{nn}}{N_{np}} = f[\Delta\theta_{12}, \Delta(T_1 + T_2), \Gamma_2] \quad (1)$$

to be valid in a situation, such as the experimental one, in which particular intervals of variability of the pair opening angle, $\Delta\theta_{12}$, and sum energy, $\Delta(T_1 + T_2)$, are employed in the determination of N_{nn} and N_{np}. Actually, as one can deduce from Figs. 1–5, not only N_{nn} and N_{np} but also the ratio N_{nn}/N_{np} depends on $\Delta\theta_{12}$ and $\Delta(T_1 + T_2)$. The numbers of nucleon pairs N_{nn}, N_{np}, and N_{pp} discussed up to now are related to the corresponding quantities for the one-nucleon ($N_{NN}^{\rm 1B}$) and two-nucleon ($N_{NN}^{\rm 2B}$) induced processes [the former (latter) being normalized per one-body (two-body) stimulated nonmesonic weak decay] via the following equation:

$$N_{NN} = \frac{N_{NN}^{\rm 1B}\Gamma_1 + N_{NN}^{\rm 2B}\Gamma_2}{\Gamma_1 + \Gamma_2}. \quad (2)$$

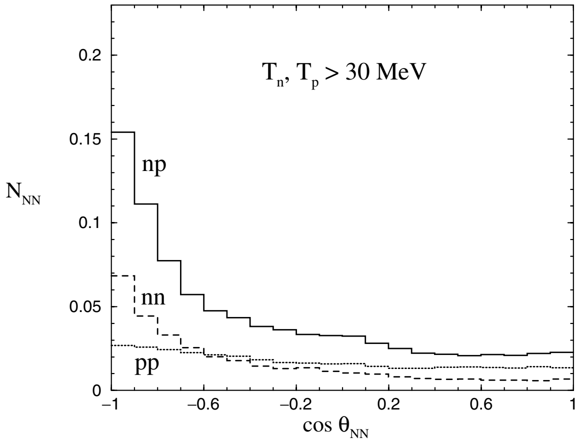

FIG. 5. Opening angle correlations of *nn*, *np*, and *pp* pairs emitted *per nonmesonic decay* of ${}^{12}_{\Lambda}$C. See text for details.

TABLE I. Results for N_{nn}, N_{np}, and N_{nn}/N_{np} corresponding to the nonmesonic decay of ${}^{12}_{\Lambda}$C. A null (30 MeV for the numbers in parentheses) nucleon energy threshold and two different opening angle regions are considered.

	$\cos\theta_{NN} \leq -0.8$	All θ_{NN}
$N_{nn}^{\rm wd}$	0.20 (0.19)	0.25 (0.24)
$N_{np}^{\rm wd}$	0.57 (0.56)	0.75 (0.72)
$N_{nn}^{\rm wd}/N_{np}^{\rm wd} \equiv \Gamma_n/\Gamma_p$	0.34 (0.34)	0.34 (0.34)
N_{nn}	0.44 (0.11)	3.15 (0.33)
N_{np}	1.05 (0.26)	8.40 (0.87)
N_{nn}/N_{np}	0.42 (0.43)	0.38 (0.39)

Table I shows the dependence of N_{nn}, N_{np}, and N_{nn}/N_{np} on $\Delta\theta_{12}$ and $\Delta(T_1 + T_2)$ for ${}^{12}_{\Lambda}$C. For comparison, the same quantities for the primary weak decay nucleons are listed as well. Without any restriction on θ_{NN} and the nucleon energies, one notes a great increase (by about 1 order of magnitude) of both the *nn* and *np* pair numbers when FSI are taken into account [24]. FSI affect especially the low energy nucleons ($T_N \leq$ 30 MeV) and the non-back-to-back *NN* kinematics ($\cos\theta_{NN} > -0.8$), as demonstrated in Table I by the reduced number of *nn* and *np* pairs when energy cuts and/or angular restrictions are applied. On the contrary, the ratio between the number of *nn* and *np* pairs is much less sensitive to FSI.

In Table II (III), the ratio N_{nn}/N_{np} for ${}^{5}_{\Lambda}$He (${}^{12}_{\Lambda}$C) is given for different combinations of opening angle interval and nucleon energy threshold. In parentheses we also report the predictions obtained when the two-nucleon induced decay channel is neglected. The results of our figures and tables are in a form that permits a direct comparison with the KEK-E462 experiment [19], whose preliminary results supply a N_{nn}/N_{np} ratio for ${}^{5}_{\Lambda}$He of about 0.5 (with an error bar of about 20%) for a kinetic energy threshold of 30 MeV and all the cases quoted in Table II but the one corresponding to the integration over

TABLE II. Predictions of N_{nn}/N_{np} for ${}^{5}_{\Lambda}$He corresponding to different nucleon thresholds $T_N^{\rm th}$ and pair opening angles. The numbers in parentheses correspond to calculations with $\Gamma_2 = 0$ in Eq. (2).

	$\cos\theta_{NN}$			
$T_N^{\rm th}$ (MeV)	≤ -0.8	≤ -0.6	≤ -0.4	All
30	0.61 (0.52)	0.61 (0.51)	0.60 (0.50)	0.54 (0.45)
50	0.63 (0.52)	0.61 (0.51)	0.60 (0.51)	0.56 (0.46)

TABLE III. Same as in Table II for ${}^{12}_{\Lambda}$C.

	$\cos\theta_{NN}$			
$T_N^{\rm th}$ (MeV)	≤ -0.8	≤ -0.6	≤ -0.4	All
30	0.43 (0.37)	0.43 (0.37)	0.43 (0.37)	0.39 (0.35)
50	0.41 (0.35)	0.40 (0.35)	0.40 (0.35)	0.38 (0.34)

the whole θ_{NN} range. We note that our results agree better with the data when the effect of the two-body induced decay is neglected. On the contrary, this comparison could also favor a Γ_n/Γ_p ratio slightly lower than the one (0.46) predicted by our OME model for ${}^{5}_{\Lambda}$He. However, it is still premature to try to clarify this point in view of the preliminary character of the KEK-E462 data. On the other hand, three-nucleon coincidences studies are necessary to disentangle the effects of one- and two-body stimulated decay channels from observed decay events. Indeed, the results of the present work clearly demonstrate that, due to the magnitude of the nucleon FSI, the simplistic picture that the back-to-back kinematics is able to select one-nucleon induced processes is far from being realistic.

In conclusion, our OME weak interaction model supplemented by FSI through an intranuclear cascade simulation provides two-nucleon coincidence observables which reproduce the preliminary KEK-E462 results for ${}^{5}_{\Lambda}$He. This allows us to conclude that Γ_n/Γ_p for ${}^{5}_{\Lambda}$He should be close to 0.46. Let us recall that all the previous experimental analyses of single nucleon spectra (see, for instance, Ref. [18]), supplemented in some cases by intranuclear cascade calculations, obtained Γ_n/Γ_p values in disagreement with pure theoretical predictions. In our opinion, the fact that our analysis permits one to reproduce (preliminary) coincidence data for a value of Γ_n/Γ_p as small as 0.46 for ${}^{5}_{\Lambda}$He could signal the existence of non-negligible interference effects between the n- and p-induced channels in the single nucleon spectra data. Therefore, although further (theoretical and experimental) confirmation is needed, in this paper we think we have proved how the study of nucleon coincidence observables can offer a promising possibility to solve the long-standing puzzle on the Γ_n/Γ_p ratio.

In a forthcoming (long) paper [25] we shall discuss the nucleon correlation observables for the (one- and two-nucleon stimulated) nonmesonic decay of ${}^{5}_{\Lambda}$He and ${}^{12}_{\Lambda}$C in a systematic way. Single nucleon spectra will be a further subject of this work. In addition, one should treat the case of ${}^{4}_{\Lambda}$He, which is of extreme importance in order to test the validity of the $\Delta I = 1/2$ isospin rule in the $\Lambda N \rightarrow nN$ weak transition [1,9,21], another key point for the solution of the Γ_n/Γ_p puzzle.

This work is partly supported by EURIDICE HPRN-CT-2002-00311, by the DGICYT BFM2002-01868, by the Generalitat de Catalunya SGR2001-64, and by INFN. Discussions with H. Outa are acknowledged.

[1] W. M. Alberico and G. Garbarino, Phys. Rep. **369**, 1–109 (2002).

[2] E. Oset and A. Ramos, Prog. Part. Nucl. Phys. **41**, 191–253 (1998).

[3] J. F. Dubach, G. B. Feldman, and B. R. Holstein, Ann. Phys. (N.Y.) **249**, 146 (1996).

[4] A. Parreño, A. Ramos, and C. Bennhold, Phys. Rev. C **56**, 339 (1997).

[5] D. Jido, E. Oset, and J. E. Palomar, Nucl. Phys. **A694**, 525 (2001).

[6] A. Parreño and A. Ramos, Phys. Rev. C **65**, 015204 (2002).

[7] K. Itonaga, T. Ueda, and T. Motoba, Phys. Rev. C **65**, 034617 (2002).

[8] A. Parreño, A. Ramos, C. Bennhold, and K. Maltman, Phys. Lett. B **435**, 1 (1998).

[9] W. M. Alberico and G. Garbarino, Phys. Lett. B **486**, 362 (2000).

[10] W. M. Alberico, A. De Pace, M. Ericson, and A. Molinari, Phys. Lett. B **256**, 134 (1991).

[11] A. Ramos, E. Oset, and L. L. Salcedo, Phys. Rev. C **50**, 2314 (1995).

[12] W. M. Alberico, A. De Pace, G. Garbarino, and A. Ramos, Phys. Rev. C **61**, 044314 (2000).

[13] W. M. Alberico, A. De Pace, G. Garbarino, and R. Cenni, Nucl. Phys. **A668**, 113 (2000).

[14] K. Sasaki, T. Inoue, and M. Oka, Nucl. Phys. **A669**, 331 (2000); **A678**, 455(E) (2000).

[15] K. Sasaki, T. Inoue, and M. Oka, Nucl. Phys. **A707**, 477 (2002).

[16] A. Ramos, M. J. Vicente-Vacas, and E. Oset, Phys. Rev. C **55**, 735 (1997).

[17] A. Ramos, M. J. Vicente-Vacas, and E. Oset, Phys. Rev. C **66**, 039903 (2002); Erratum of Ref. [16].

[18] A. Montwill *et al.*, Nucl. Phys. **A234**, 413 (1974); J. J. Szymanski *et al.*, Phys. Rev. C **43**, 849 (1991).

[19] H. Outa *et al.*, KEK Report No. KEK-PS E462, 2000; (private communication).

[20] A. Feliciello, Nucl. Phys. **A691**, 170c (2001); P. Gianotti, Nucl. Phys. **A691**, 483c (2001).

[21] R. L. Gill, Nucl. Phys. **A691**, 180c (2001).

[22] V. G. J. Stoks and T. A. Rijken, Phys. Rev. C **59**, 3009 (1999).

[23] The values of Γ_2/Γ_1 used in this paper have been obtained with the method of Ref. [12] after correcting a small (conceptual) error in the implementation of data on the P-wave pion-nucleus optical potential. For ${}^{5}_{\Lambda}$He and ${}^{12}_{\Lambda}$C, such a correction slightly decreases the values of Γ_1 while increasing Γ_2 by about 20%.

[24] Note that, because of the mentioned eventuality that the Monte Carlo code could provide nonrealistic results for small energy thresholds, the results presented in Table I for a null threshold should be considered as being only qualitative.

[25] G. Garbarino, A. Parreño, and A. Ramos (to be published).